Chinese Medical Journal®

Clinicopathological characteristics and genetic alterations in clear cell carcinoma cells derived from Mullerian duct epithelium of the prostate

Shaoan Chen[1], Fengyun Cui[2], Peizhi Zhang[3], Li Chen[4], Wei Song[1], Qingchao Meng[5], Xiude Chen[1], Qinghua Xia[1], Weiting Kang[1]

[1]Department of Urology, Shandong Provincial Hospital Affiliated to Shandong First Medical University, Jinan, Shandong 250021, China;
[2]Department of Pathology, Shandong Provincial Hospital Affiliated to Shandong First Medical University, Jinan, Shandong 250021, China;
[3]Department of Urology, Shandong Provincial Hospital, Cheeloo College of Medicine, Shandong University, Jinan, Shandong 250021, China;
[4]Department of Medical Ultrasound, Shandong Provincial Hospital Affiliated to Shandong First Medical University, Jinan, Shandong 250021, China;
[5]Department of Radiology, Shandong Provincial Hospital Affiliated to Shandong First Medical University, Jinan, Shandong 250021, China.

Müllerian duct cysts of the prostate, which are common in young men, are relatively rare clinical complications. Moderately large cysts present with urinary obstruction, urinary tract irritation, subsequent frequent urination, urgency, and dysuria. Larger cysts can compress the seminal vesicles or ejaculatory ducts and cause intractable bloody sperms or obstructive azoospermia. Malignant transformation of Müllerian duct cysts is even rarer. Only 10 cases of Müllerian duct malignancies have been reported in previous studies.[1-9] We reported a case of one patient admitted to our center and discussed the clinicopathologic features, diagnosis, treatment, and prognosis of the disease based on literature data. In addition, we performed whole-exome sequencing and analysis of pathological tissues, screened the mutant genes of clear cell carcinoma of Müllerian duct cyst, and preliminarily discussed its pathogenesis.

This study was approved by the Ethics Committee of Shandong Provincial Hospital (Jinan, China; SWYX: No. 2022-132). A 30-year-old male presented at our hospital with 6 years of intermittent hematospermia without urinary obstruction and urinary tract irritation. Digital rectal examination revealed a tough cyst-like mass between the rectum and bladder, but without discharge from the urethra. Expressions of various tumor markers, such as total prostate-specific antigen(tPSA) (0.558 ng/mL, reference value: 0–5 ng/mL), were within normal ranges. Sex hormone levels were also within normal ranges. Semen analysis revealed that sperm density and total sperm count was 0. B-ultrasound showed a cystic solid mass of about 5.8 cm ×3.9 cm ×3.1 cm and a denser inner solid section of about 4.1 cm ×2.9 cm ×1.6 cm. Enhanced magnetic resonance imaging (MRI) of the pelvic region revealed an irregular cystic solid mass of about 4.0 cm ×4.8 cm ×6.4 cm on the left side of the seminal vesicle gland. The solid mass generated mixed long and short T1 as well as long and short T2 signals. Diffusion-weighted imaging and apparent diffusion coefficient revealed poor local diffusions. Under enhanced scanning, the solid part of the mass was irregular and progressive, while the boundary between the cystic mass and prostate was not clear [Figure 1A]. Positron emission tomography–computed tomography revealed that the increase in 18F-fluorodeoxyglucose metabolism in the left seminal vesicle gland mass was not significant while the boundary between the cystic mass and prostate was not clear.

After obtaining informed consent from the patient, robot-assisted laparoscopic radical prostatectomy (extraperitoneal) was performed for complete resection of the lesion. Seven days after surgery, the urinary catheter was removed, and the patient had a good urinary control. After opening up the prostate glands, the cyst, which was about 5.0 cm × 4.0 cm × 4.0 cm in size, was clearly visible. Its wall was slightly rough and the thickness was about 0.2 to 0.5 cm. The dark-pink area of the solid nodules was about 2.5 cm ×2.0 cm and broken [Figure 1B]. Under low-power magnification, capsule walls were thick with clear boundaries. The solid cyst duct, adenoid, and papillary

Access this article online

Quick Response Code:

Website: www.cmj.org

DOI: 10.1097/CM9.0000000000002252

Correspondence to: Weiting Kang, Department of Urology, Shandong Provincial Hospital Affiliated to Shandong First Medical University, Jinan, Shandong 250021, China
E-Mail: weiting_kang@163.com

Chinese Medical Journal 2022;135(20)

Received: 21-04-2022; **Online:** 07-11-2022 **Edited by:** Yanjie Yin and Xiuyuan Hao

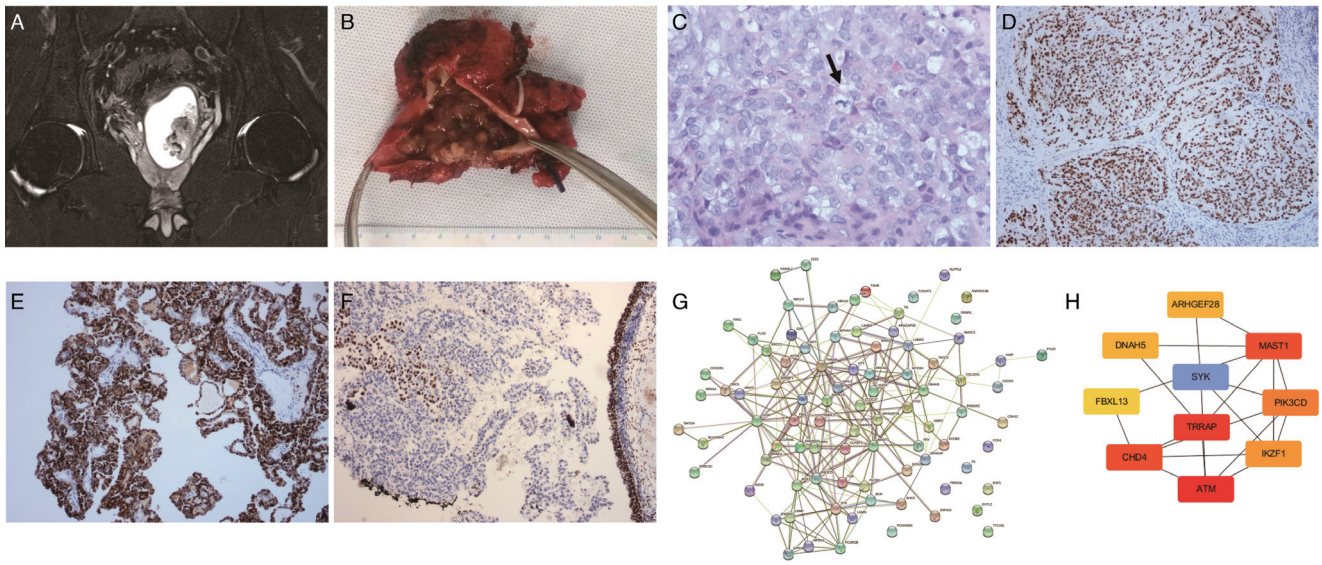

Figure 1: (A) The magnetic resonance imaging T2 phase of the prostate from the coronal position. (B) The resected tumor mass. (C) Hematoxylin-eosin staining revealed that the tumor was arranged into solid, cystic duct, and adenoid and papillary structures; further, the cells lining the surface was found to be spike-like on 100× magnification. (D) Expressions of paired box gene 8 (PAX8) proteins in tumor cells. The image was captured at 100× magnification. (E) Cytoplasmic expressions of Napsin A in tumor cells. The image was captured at 100× magnification. (F) Focal expressions of estrogen receptor (left), and residual epithelium of the Müllerian duct (right), under 100× magnification. (G) PPI network of proteins coded by mutant genes in Müllerian duct adenocarcinoma tissues. (H) Hub genes in the PPI network. PPI: Protein–protein interaction.

structures were observed in the tumor parenchyma. The residual Müllerian duct epithelium was on the inner part of the local cyst wall, whereas prostate glands were on the outer part of the wall. Under high magnification, the solid mass was found to be rich in transparent adenoid cells and a few eosinophils with big nuclei, and numerous atypical cells were present and most of them were actively divided [Figure 1C]. Capsular and papillary structures were surrounded with a single layer of spike-like cells, with acidophilic or transparent cytoplasm. Immunohistochemical analysis revealed strong expressions of Paired box gene 8 [Figure 1D] in tumor cells. Immunohistochemical staining showed that Napsin A was mainly present in the cytoplasm, and the staining was diffuse and strongly positive [Figure 1E]. Focal expressions of estrogen receptor (ER) were mid-intensity nuclear positive in tumor cells, and Müllerian duct residual epithelium was diffuse and strongly positive [Figure 1F]. Expressions of androgen receptor, prostate-specific antigen, cluster of differentiation 10, vimentin, and keratin 20 were not detected.

Post-operative samples were subjected to immunohistochemistry and whole-exome sequencing. There were 95 gene mutations [Supplementary Table 1, http://links.lww.com/CM9/B123], including ataxia telangiectasia mutated (ATM) p.Gln118Ter (with a mutation frequency of 6.0%) and excision repair cross-complementation group 2 p.Val10Leu (with a mutation frequency of 6.7%) in the Müllerian duct adenocarcinoma tissues. The top 20 genes with the highest mutation frequencies were SPARC-related modular calcium-binding protein 2 (*SMOC2*), dynein axonemal heavy chain 5 (*DNAH5*), tetratricopeptide repeat domain 23 like, chromodomain helicase DNA binding protein 4 (*CHD4*), mitogen-activated protein kinase 15, alkaline phosphatase placental-like 2, GRAM domain containing 4, chromosome 10 open reading frame 71, G protein-coupled receptor 183, transmembrane protein 88B, potassium voltage-gated channel subfamily B member 2, FANCD2 and FANCI associated nuclease 1, cytoplasmic linker associated protein 1, protocadherin gamma subfamily B, 3, ATP binding cassette subfamily A member 2, Fc gamma receptor IIb, striated muscle preferentially expressed protein kinase, leucine rich repeat containing 56, phospholipase C beta 3, and Keratin 1 [Supplementary Figure 1, http://links.lww.com/CM9/B123]. Gene copy number variations and gene rearrangements were not detected. A potential germline pathogenic variant in the BLM RecQ like helicase (*BLM*) gene was also detected. The Hereditary tumor risk indicates that the BLM P.Tyr430Ter mutation related to tumor genetic susceptibility may be a pathogenic mutation. The tumor mutation burden (TMB) was 3.12 muts/Mb, while the tumor microsatellite was stable.

As shown in Supplementary Figure 2A–C, http://links.lww.com/CM9/B123, gene ontology analysis revealed that the 95 mutated genes were enriched in several biological processes, including vesicle targeting, neutrophil degranulation, cytoskeleton organization, and system development; the enriched cellular components included spindles, protein complex, plasma membrane proteins, organelles, and microtubules, while the enriched molecular functions included ribonucleotide binding, binding of purines to ribonucleotides, binding of purine ribonucleosides to the triphosphate, protein complex binding, and protein binding. Kyoto Encyclopedia of Genes and Genomes analysis revealed that the 95 mutated genes regulate vascular endothelial growth factor signaling, lipolysis in adipocytes, prolactin signaling, phosphoinositide 3-kinase/protein kinase B signaling, nuclear factor κ-light-chain-enhancer of activated B cells signaling,

natural killer cell-mediated cytotoxicity, and cyclic adenosine monophosphate signaling [Supplementary Figure 2D, http://links.lww.com/CM9/B123].

Protein–protein interaction (PPI) of mutant genes [Figure 1G] revealed that, the number of edges was 87; the average node degree was 219; the average local clustering coefficient was 5.03; and the expected number of edges was 0.314, while the PPI enrichment *P* value was 0.00669. Hub genes [Figure 1H] in the PPI network were *ATM*, transformation/transcription domain associated protein, microtubule associated serine/threonine kinase 1, CHD4, phosphatidylinositol 4,5-bisphosphate 3-kinase catalytic subunit delta isoform, ikaros family zinc finger protein 1, Rho guanine nucleotide exchange factor 28, DNAH5, and F-box and leucine rich Repeat protein 13.

This is a rare study to perform full exome sequencing and sequencing-based post-operative medication guidance for Müllerian tube-derived malignant tumors. *SMOC2*, a tumor suppressor in colorectal and thyroid cancers, is associated with better prognostic outcomes for patients. In prostate cancer, *ATM* mutations can lead to a blockade of DNA damage repair, causing cell cycle abnormalities, thereby promoting tumorigenesis. *BLM* mutations are associated with a risk of Bloom syndrome, with an autosomal recessive inheritance pattern. In this case, *BLM p.Tyr430Ter* was detected as heterozygous, implying that the patient is only a carrier of the pathogenic mutation site. Findings from gene sequencing in this study provide a molecular basis for in-depth studies on the occurrence and development of clear cell carcinoma of Müllerian in the prostate. The mutation frequency of *ATM p.Gln118Ter* was 6.0%, suggesting that the patients may benefit from olaparib, niraparib, rucaparib, talazoparib, fluzoparib, and pamiparib. Given the TMB of 3.12, the patients may not benefit from the administration of immune checkpoint inhibitors alone. Half a year after surgery, the patient is in good condition and is under continuous follow-up.

In summary, clinical incidences of Müllerian duct malignancies in the prostate are extremely low, while the appropriate diagnostic and treatment strategies have not been fully established. Diagnosis can be done by imaging examinations, such as magnetic resonance imaging (MRI), seminal vesiclescopy, and biopsy. The most common surgical approach is tumor resection or radical prostatectomy by open surgery or laparoscopy. Gene sequencing analysis can provide a reference value for post-operative adjuvant treatment of such cases. The disease requires long-term follow-up to assess its prognosis.

Funding

This work was partly supported by a grant from the Natural Science Foundation of China (No. 81072200).

Conflicts of interest

None.

References

1. Szemes GC, Rubin DJ. Squamous cell carcinoma in a Müllerian duct cyst. J Urol 1968;100:40–43. doi: 10.1016/s0022-5347(17)62469-8.
2. Hodgson NB. Long-term survival from Müllerian duct carcinoma. J Urol 1976;116:313–315. doi: 10.1016/S0022-5347(17)58795-9.
3. Novak RW, Raines RB, Sollee AN. Clear cell carcinoma in a Müllerian duct cyst. Am J Clin Pathol 1981;76:339–341. doi: 10.1093/ajcp/76.3.339.
4. Gilbert RF, Ibarra J, Tansey LA, Shanberg AM. Adenocarcinoma in a Müllerian duct cyst. J Urol 1992;148:1262–1264. doi: 10.1016/s0022-5347(17)36880-5.
5. Kato S, Ito H, Kobayashi K. Squamous cell carcinoma in a Müllerian duct cyst: report of a case. Surg Today 1996;26:645–648. doi: 10.1007/bf00311673.
6. Shinmura Y, Yokoi T, Tsutsui Y. A case of clear cell adenocarcinoma of the Müllerian duct in persistent Müllerian duct syndrome: the first reported case. Am J Surg Pathol 2002;26:1231–1234. doi: 10.1097/00000478-200209000-00014.
7. Warmann SW, Vogel M, Wehrmann M, Scheel-Walter HG, Artlich A, Pereira PL, *et al*. Giant mullerian duct cyst with malignant transformation in 15-year-old boy. Urology 2006;67:e423–e424. doi: 10.1016/j.urology.2005.09.009.
8. Xing JP, Dang JG, Wu DP, Long QZ, Chen XF, Nan XY. Papillary cystadenocarcinoma in a Müllerian duct cyst: report of a case with literature review (in Chinese). Natl J Androl 2006;12:218–221. doi: 10.13263/j.cnki.nja.2006.03.008.
9. Wen ZH, Zhang XH, Wei HM. Müllerian-type clear cell adenocarcinoma in male: report of a case (in Chinese). Chin J Pathol 2018;47:63–65. doi: 10.3760/cma.j.issn.0529-5807.2018.01.014.

How to cite this article: Chen S, Cui F, Zhang P, Chen L, Song W, Meng Q, Chen X, Xia Q, Kang W. Clinicopathological characteristics and genetic alterations in clear cell carcinoma cells derived from Mullerian duct epithelium of the prostate. Chin Med J 2022;135:2488–2490. doi: 10.1097/CM9.0000000000002252